

# Unconventional superconducting gap in NaFe<sub>0.95</sub>Co<sub>0.05</sub>As observed by angle-resolved photoemission spectroscopy

Z.-H. Liu,<sup>1</sup> P. Richard,<sup>2,3</sup> K. Nakayama,<sup>4</sup> G.-F. Chen,<sup>1</sup> S. Dong,<sup>1</sup> J.-B. He,<sup>1</sup> D.-M. Wang,<sup>1</sup> T.-L. Xia,<sup>1</sup> K. Umezawa,<sup>4</sup> T. Kawahara,<sup>4</sup> S. Souma,<sup>3</sup> T. Sato,<sup>4,5</sup> T. Takahashi,<sup>3,4</sup> T. Qian,<sup>2</sup> Yaobo Huang,<sup>2</sup> Nan Xu,<sup>2</sup> Yingbo Shi,<sup>2</sup> H. Ding,<sup>2</sup> and S.-C. Wang<sup>1,\*</sup>

<sup>1</sup>Department of Physics, Renmin University, Beijing, 100872, China

<sup>2</sup>Beijing National Laboratory for Condensed Matter Physics, Institute of Physics, Chinese Academy of Sciences, Beijing 100190, China

<sup>3</sup>WPI Research Center, Advanced Institute for Material Research, Tohoku University, Sendai 980-8577, Japan

<sup>4</sup>Department of Physics, Tohoku University, Sendai 980-8578, Japan

<sup>5</sup>TRiP, Japan Science and Technology Agency (JST), Kawaguchi 332-0012, Japan

(Received 6 June 2011; revised manuscript received 18 July 2011; published 23 August 2011)

We have performed high-resolution angle-resolved photoemission measurements on superconducting electron-doped NaFe<sub>0.95</sub>Co<sub>0.05</sub>As ( $T_c \sim 18$  K). We observed a holelike Fermi surface around the zone center and two electronlike Fermi surfaces around the  $M$  point, which can be connected by the  $Q = (\pi, \pi)$  wave vector, suggesting that scattering over the near-nested Fermi surfaces is important in this 111 pnictide. Nearly isotropic superconducting gaps with sharp coherent peaks are observed below  $T_c$  on all three Fermi surfaces. Upon increasing temperature through  $T_c$ , the gap size shows little change while the coherence vanishes. Large ratios of  $2\Delta/k_B T_c \sim 8$  are observed for all the bands, indicating a strong coupling in this system. These results are not expected from a classical phonon-mediated pairing mechanism.

DOI: 10.1103/PhysRevB.84.064519

PACS number(s): 74.25.Jb, 71.20.-b, 74.20.Rp, 74.70.Xa

## I. INTRODUCTION

The superconducting (SC) energy gap is one of the most important quantities in revealing the pairing mechanism of superconductors. Conventional BCS superconductors have  $s$ -wave SC gaps ( $\Delta$ ) with a  $2\Delta/k_B T_c \sim 3.5$  ratio, a characteristic of phonon-mediated pairing in the weak-coupling regime. In contrast, high- $T_c$  cuprate superconductors have an anisotropic  $d$ -wave gap with a much larger  $2\Delta_0/k_B T_c$  ratio. The discovery of a new class of high- $T_c$  superconductors in Fe pnictides<sup>1</sup> with many unconventional properties raises the question of a novel pairing mechanism in these materials. Due to the complexity of these multiband systems, literature contains many contradicting theoretical<sup>2-4</sup> and experimental results<sup>5-10</sup> about the SC gap symmetry. Penetration depth, NMR, and thermal-conductivity studies reported the possible existence of gap nodes or large variations in the gap size in pnictides.<sup>7-10</sup> There are also controversial results on the temperature dependence of the SC gap.<sup>11,12</sup> No consensus has been reached yet on the SC gap symmetry and the pairing mechanism in iron-based superconductors.

Angle-resolved photoemission spectroscopy (ARPES) is a powerful tool in directly probing the low-energy states of superconductors in the momentum ( $k$ ) space. It allows a direct band-selective measurement of the size and  $k$  profile of the SC gap. ARPES measurements on Fe-based 122,<sup>13,14</sup> 11,<sup>15</sup> and 1111 (Ref. 16) systems indicate isotropic nodeless gaps and pairing strengths in the strong coupling regime ( $2\Delta/k_B T_c \sim 5-7$ ). Among theoretical models promoted to explain these results, antiferromagnetic (AF) fluctuations have been regarded as a major candidate for pairing. Compared to other families of Fe-based superconductors, the 111 family has weaker magnetic correlations.<sup>17</sup> Recently, the consistency of the ARPES measurements on various families of Fe-based superconductors has been challenged by an ARPES report on the LiFeAs system (111).<sup>18</sup> A weak-coupling pairing

mechanism was proposed based on the observation of a  $2\Delta/k_B T_c \sim 3.1$  ratio.<sup>18,19</sup>

Here, we report ultra-high-resolution ARPES measurements on the electron-doped 111 pnictide NaFe<sub>0.95</sub>Co<sub>0.05</sub>As ( $T_c \sim 18$  K). We observed one holelike Fermi surface (FS) centered at the zone center ( $\Gamma$ ), quasinested to two elliptical FSs centered at the  $M$  point ( $\pi, \pi$ ), defined here in the unfolded Brillouin zone. Signatures of an additional small hole pocket at  $\Gamma$  are also observed. The FSs nearly have isotropic gaps with variations smaller than  $\pm 0.5$  meV. These results are consistent with an  $s_{\pm}$  symmetry<sup>16,20</sup> and exclude the possibility of symmetries with nodes. All gaps on hole and electron FSs have sizes of  $\sim 6$  to  $7$  meV, leading to a  $2\Delta/k_B T_c \sim 8$  ratio. The temperature dependence of the SC quasiparticles is similar to that of underdoped high- $T_c$  cuprates. Our results point toward unconventional superconductivity in the 111 family of Fe-based superconductors.

## II. MATERIAL AND EXPERIMENTAL SETUP

High-quality single crystals of NaFe<sub>1-x</sub>Co<sub>x</sub>As ( $x \approx 0.05$ ) with bulk  $T_c = 18$  K ( $\Delta T_c = 1$  K) were synthesized by the flux method.<sup>21</sup> Cleavage is expected to occur between the two weakly bonding Na layers, leaving a nonpolar and nonreconstructed surface. This reinforces the reliability of the ARPES results on the 111 family in characterizing the properties of the bulk. Samples (about  $1 \times 1$  mm<sup>2</sup>) were prepared in a gas-protected glove box to prevent a reaction with moisture and were cleaved *in situ*, yielding flat mirrorlike (001) surfaces. ARPES measurements were performed at Tohoku University using a Scienta 2002 analyzer with a helium-discharging lamp (He-I $\alpha$  line,  $h\nu = 21.2148$  eV) and at the Synchrotron Radiation Center (Madison, WI), using a Scienta R4000 analyzer. We performed experiments within the 4–100-K temperature range in a vacuum better than  $4 \times 10^{-11}$  Torr. No noticeable aging was observed during each

measurement cycle. The energy resolution used for measuring fine features was better than 3 meV.

### III. RESULTS AND DISCUSSIONS

Energy distribution curves (EDCs) along  $(0,0)-(\pi,\pi)(\Gamma-M)$  in the normal state ( $T = 30$  K) of an optimally doped  $\text{NaFe}_{0.95}\text{Co}_{0.05}\text{As}$  sample are plotted in Fig. 1(a). To enhance the band dispersion, the EDCs close to  $\Gamma$  along the  $M-\Gamma$  direction are plotted in the inset of Fig. 1(a). Three bands are seen and are marked close to  $E_F$  around  $\Gamma$ . The summary of the band dispersion along that high-symmetry line is given in Fig. 1(d). We identify three holelike bands around the  $\Gamma$  point, named  $\alpha$ ,  $\alpha'$ , and  $\beta$ , respectively. Only the  $\alpha$  band clearly crosses  $E_F$ . According to local-density approximation calculations,<sup>22</sup> there exist three holelike bands around  $\Gamma$ . Two bands ( $\alpha$ ,  $\alpha'$ ) are degenerate at  $\Gamma$  at an energy higher than the third one ( $\beta$ ). Following this

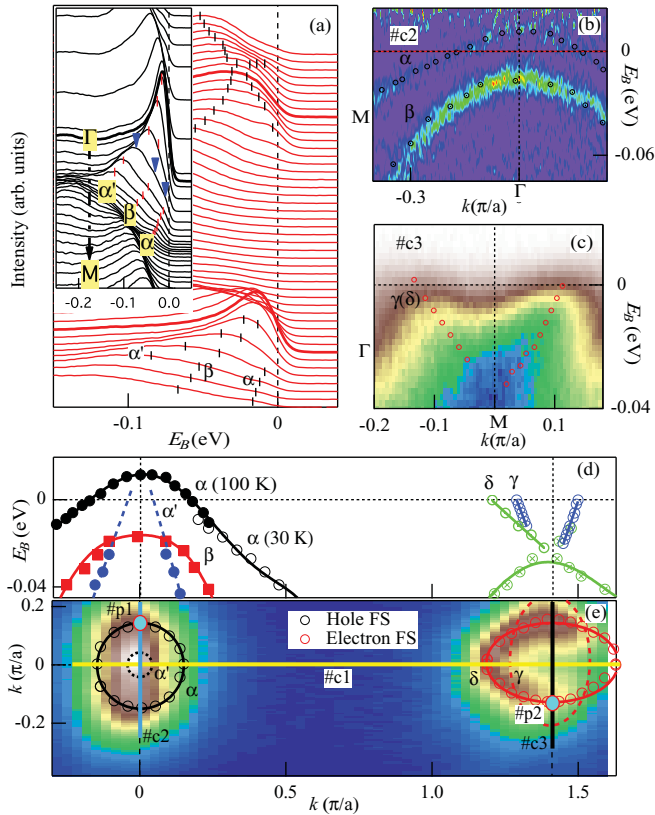


FIG. 1. (Color online) (a) EDCs of  $\text{NaFe}_{0.95}\text{Co}_{0.05}\text{As}$  in the normal state ( $T = 30$  K) cut #c1 in (e). Insets are EDCs around  $\Gamma(0,0)$ . Ticks are used to mark band dispersions. (b) Second derivative  $[\partial^2 I(\omega, k)/\partial \omega^2]$  of intensity along cut #c2 in (e) at  $T = 100$  K. The Fermi function was divided out to enhance the band dispersion above  $E_F$ . Markers are extracted band dispersions serving as a guide to the eye. (c) Normal state photoemission intensity along cut #c3 indicated in (e) ( $T = 30$  K). (d) Extracted band dispersions from (a)–(c). Blue dashed lines are the linear extrapolation of the  $\alpha'$  band. (e) Integrated intensity ( $\pm 5$  meV) around  $E_F$  as a function of  $(k_x, k_y)$ . Open circles are extracted FSs. Solid lines are fitted FSs, while the black dashed circle is obtained from the linear extension of the  $\alpha'$  band to  $E_F$ , and the red dashed ellipse is a  $90^\circ$  rotation of the  $\gamma(\delta)$  FS with respect to the  $M$  point.

scheme, we assume that the second band ( $\alpha'$ ) crosses  $E_F$  and overlaps with the  $\alpha$  band at the  $\Gamma$  point. In order to determine the top of the  $\alpha$  band, we show the second-derivative intensity plot along  $(0,0)-(-\pi,\pi)(\Gamma-M')$  at an elevated temperature ( $T = 100$  K) in Fig. 1(b). The Fermi function was divided out to unmask the band dispersion above  $E_F$ . Here, the  $\alpha$  band crosses  $E_F$  at  $k_F \sim 0.15\frac{\pi}{a}$ , and the band top is at 10–15 meV above  $E_F$ . The third band ( $\beta$ ) sinks 10–15 meV below  $E_F$ .

The EDCs in Fig. 1(a) exhibit a clear electronlike band in the vicinity of  $M$ . For the perpendicular direction, as indicated by #c3 in panel (e), the intensity plot displayed in Fig. 1(c) shows an electronlike band crossing  $E_F$  with a slightly different  $k_F$  value. We refer to them as the  $\gamma$  and  $\delta$  bands.

Figure 1(e) summarizes the FS topology of this material: one large circular holelike FS ( $\alpha$ ), possibly a smaller one ( $\alpha'$ ) around  $\Gamma$ , and two elliptical electronlike FSs ( $\gamma, \delta$ ) around  $M$ . The band arrangement and FS surface topology are consistent with a report on the undoped  $\text{NaFeAs}$  parent compound.<sup>23</sup> We estimate that the net-enclosed FS area [with electron-(hole-) like FSs counted as positive (negative) values] is about  $4.3 \pm 1.2\%$  of the whole Brillouin zone, in agreement with the nominal bulk-electron concentration of 5% per Fe atom. As with the 122 pnictides for which Co substitution is accompanied by a chemical potential shift due to doping,<sup>24</sup> the Co substitution in  $\text{NaFe}_{1-x}\text{Co}_x\text{As}$  induces extra free electrons into the system, in agreement with neutron and muon measurements.<sup>25</sup> Even though AF fluctuations in this material were reported to be weaker than in other pnictides,<sup>17</sup> our results indicate that the  $\alpha$  and  $\gamma(\delta)$  FSs can be connected fairly well by the  $Q = (\pi, \pi)$  AF wave vector, suggesting strong inter-FS scattering in this material.<sup>2,26–29</sup>

As illustrated by the EDCs given in Fig. 2, the quasiparticle peaks become sharper in the vicinity of  $E_F$ , and a SC gap opens at  $k_F$  when the temperature decreases below  $T_c$ . Interestingly, the peaks at  $k_F$  are as sharp as the peaks observed in  $\text{LiFeAs}$ ,<sup>18</sup> indicating that possible scattering by Co dopants does not affect the lifetime of the quasiparticles significantly. The symmetrized EDCs at  $k_F$ , measured at different temperatures, are plotted in Figs. 3(a) and 3(b). Assuming particle-hole symmetry, symmetrization allows us to approximately remove the effect of the Fermi-Dirac function at  $k_F$ . From the symmetrized EDCs, we observe sharp quasiparticle peaks below  $E_F$ , with a well-defined gapped region between the two peaks. We define the SC gap value  $\Delta(T)$  as half the distance between the two SC coherent peaks in the symmetrized EDCs. At low temperatures, we observe a peak-peak distance of  $\sim 13$  meV. As temperature increases, the coherent peak intensity decreases steadily and becomes vanishingly small about  $5 \sim 10$  K above  $T_c$ . The gapped region between the coherent peaks fills up and disappears at the same temperature as the peak vanishes.

For a more quantitative analysis of the temperature evolution of the SC gap, we used the formula suggested by Norman *et al.* describing the self-energy  $\Sigma(k, \omega)$  of quasiparticles in the SC state:<sup>30</sup>  $\Sigma(k, \omega) = -i\Gamma + \Delta^2/[(\omega + i0^+) + \epsilon(k)]$ , where  $\Delta$  is the gap size and  $\Gamma$  is the single-particle scattering rate simplified as  $\omega$  independent. Assuming a polynomial background, this function fits the spectral line shape remarkably well at different temperatures until the peak vanishes, as illustrated in Fig. 3(c). The extracted gap

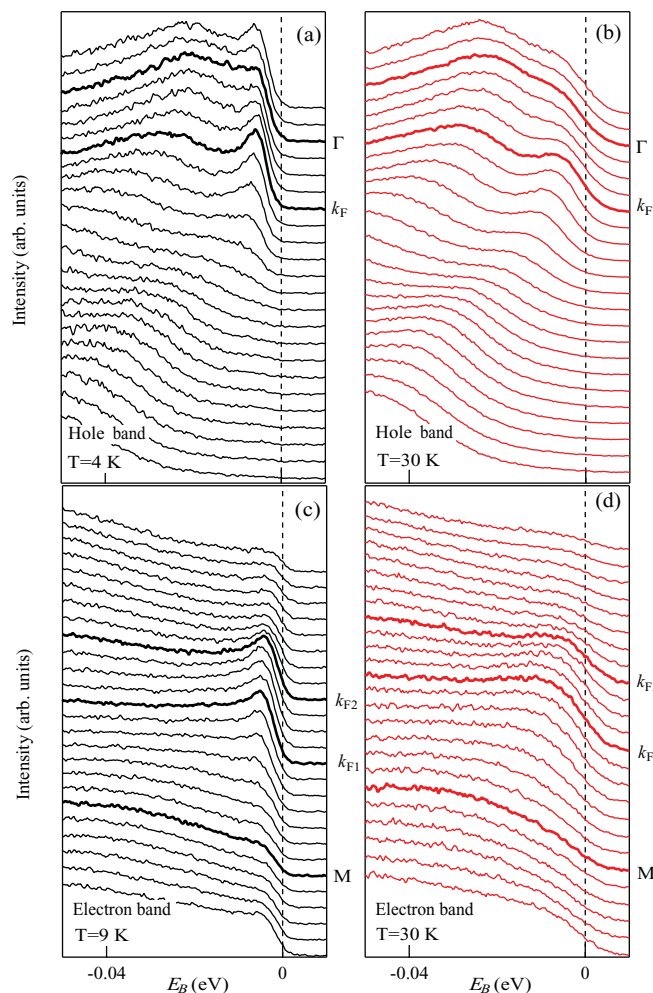


FIG. 2. (Color online) (a) and (b) Dispersive EDCs along cut #2 in Fig. 1(e) measured below (a) and above (b)  $T_c$ . (c) and (d) Dispersive EDCs along cut #3 in Fig. 1(e) measured below (c) and above (d)  $T_c$ . High-symmetry points ( $\Gamma$  and  $M$ ) and band crossing points are identified.

sizes and coherent peak linewidths for the hole and electron bands are shown in Figs. 3(d) and 3(e), respectively. We observe that the gaps change little with increasing temperature and persist even above  $T_c$ . The linewidth ( $\Gamma$ , defined as the half width at half maximum), which is proportional to the scattering rate, also changes little with temperature. On the other hand, the normalized coherent weight, defined as the integrated area  $Z_A = \int A_{\text{coh}}(k, \omega) d\omega / \int A(k, \omega) d\omega$  following the same procedure as in earlier works for the cuprates,<sup>31,32</sup> has a strong temperature dependence. As temperature increases,  $Z_A$  decreases and approaches zero slightly above the bulk  $T_c$ .

This unusual temperature evolution in  $\text{NaFe}_{0.95}\text{Co}_{0.05}\text{As}$  is different from the gap-closing behavior of a conventional BCS superconductor and is similar to what has been observed in the underdoped cuprates,<sup>30</sup> suggesting unconventional superconductivity in this pnictide superconductor. The observation of a coherence peak with an energy gap above  $T_c$  is unusual in iron pnictides. Possibly, it could be due to the existence of a pseudogap with a crossover temperature ( $T^*$ ) about 5 ~ 10 K above  $T_c$ . Recently, an ARPES measurement

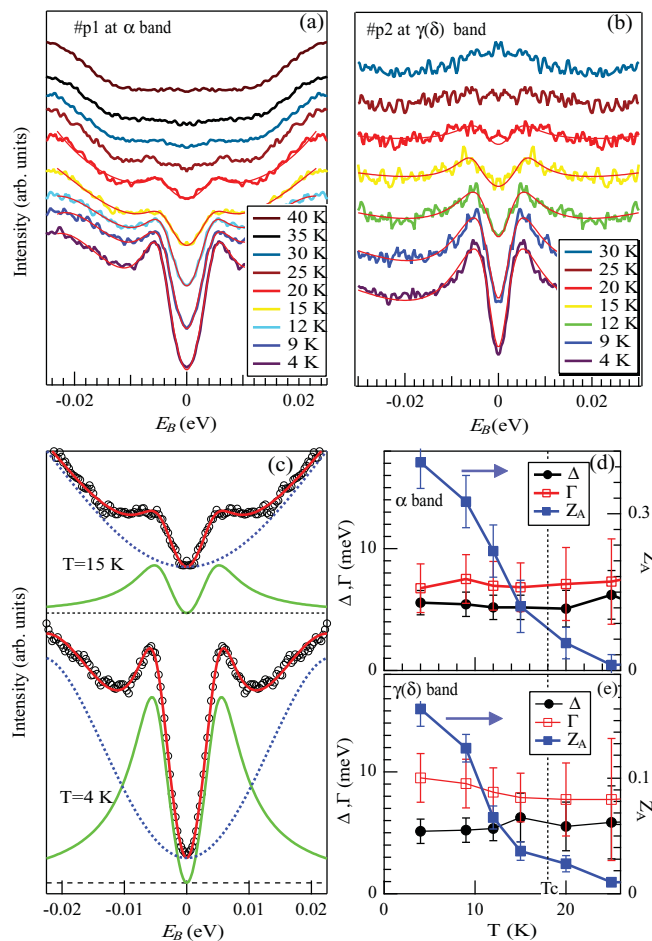


FIG. 3. (Color online) (a) and (b) Temperature dependence of the spectra at  $k_F$  of the  $\alpha$  [#p1 in Fig. 1(e)] and  $\gamma(\delta)$  [#p2 in Fig. 1(e)] bands, respectively. (c) Fitting examples of symmetrized EDC spectra of the  $\alpha$  band. Green lines correspond to  $A(k, \omega)$  (see the text), whereas, dashed blue lines refer to a polynomial background. The fitted results are indicated by the red lines. (d) and (e) Temperature dependence of the quasiparticle properties extracted from data in panels (a) and (b), respectively.  $Z_A$  is the normalized coherent area given by  $Z_A = \int A_{\text{coh}}(\omega) / A(\omega) d\omega$  in the  $\pm 20$ -meV energy range.

on  $\text{Ba}_{1-x}\text{K}_x\text{Fe}_2\text{As}_2$  reported a pseudogap coexisting with a superconducting gap in the underdoped region and was possibly driven by AF fluctuations.<sup>33</sup> An alternative scenario is that the transition temperature at the surface, where the mobile Na concentration may be different from the bulk, is slightly higher than the one in the bulk.

We have performed high-resolution measurements of the  $k$  dependence of the SC gap for the  $\alpha$  and  $\gamma(\delta)$  bands. EDCs at various  $k_F$ 's along the  $\alpha$  and  $\gamma(\delta)$  FSs are plotted in Figs. 4(a) and 4(b), respectively, and the corresponding extracted SC gap sizes at low temperatures are plotted as a function of the polar angle in Figs. 4(c) and 4(d), respectively. In all cases, the coherent peaks are located about 6 to 7 meV below  $E_F$ , with a  $k$  variation smaller than  $\pm 0.5$  meV. These values lead to  $2\Delta/k_B T_c \sim 8$  to 9. Even assuming a higher surface  $T_c$  ( $\sim 25$  K), the reduced ratio ( $2\Delta/k_B T_c \sim 6$ ) remains in the strong coupling region. Similar to the 122-system  $\text{Ba}_{0.6}\text{K}_{0.4}\text{Fe}_2\text{As}_2$ ,<sup>13,34</sup> the absence of a gap node or large

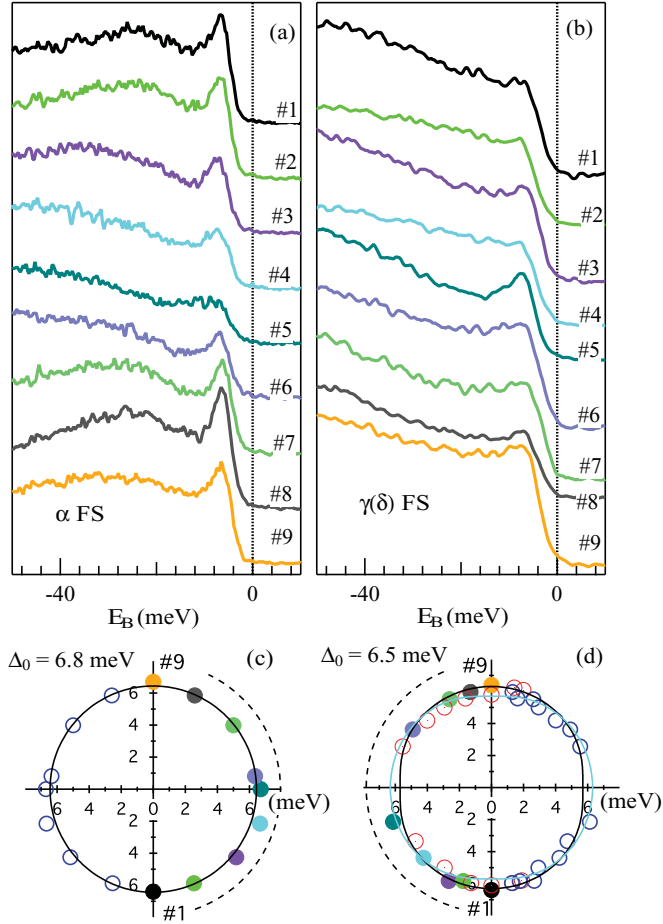


FIG. 4. (Color online) (a) and (b) Low-temperature EDCs along the  $\alpha$  and  $\gamma(\delta)$  FSs, respectively. (c) and (d) Corresponding extracted gap sizes plotted in polar coordinates with respect to each FS center. The colors of the solid circles and the label numbers refer to the corresponding colors and labels of the EDCs in (a) and (b). Open red circles correspond to additional extracted values not shown in (b), while blue circles are obtained by symmetry operations. Black lines are  $\Delta(s_{\pm}) = \Delta_0 |\cos k_x \cos k_y|$  fits, with  $\Delta_0 = 6.8$  meV for the  $\alpha$  band and  $\Delta_0 = 6.5$  meV for the  $\gamma(\delta)$  band.

variation in the gap size on all the FSs in  $\text{NaFe}_{0.95}\text{Co}_{0.05}\text{As}$  excludes the possibility of symmetries with in-plane nodes, such as the  $d$  wave. In Figs. 4(c) and 4(d), the solid lines indicate fits to the simple  $s_{\pm}$ -wave gap function of  $\Delta_0 |\cos k_x \cos k_y|$ ,<sup>35</sup> with  $\Delta_0 = 6.8$  and 6.5 meV for the hole and electron FSs, respectively.

Using the leading-edge shift across  $T_c$  to define the SC gap size, a recent ARPES study on  $\text{LiFeAs}$  (Ref. 18) claimed a much smaller  $2\Delta/k_B T_c \sim 3.5$  ratio, close to the BCS limit, and suggested weak-coupling superconductivity in  $\text{LiFeAs}$ .  $\text{LiFeAs}$  is nonmagnetic and has a smaller As-Fe-As angle, which might be different from other strongly coupled Fe-based superconductors. Another possibility involves the higher mobility of the Li atoms on the surface as compared to Na in the isostructural  $\text{NaFe}_{0.95}\text{Co}_{0.05}\text{As}$  compound, which may lead to a different stoichiometry on the surface. In addition, the leading-edge shift may likely underestimate the SC gap size, which, in turn, would yield a smaller  $2\Delta/k_B T_c$  ratio. In  $\text{NaFe}_{0.95}\text{Co}_{0.05}\text{As}$ , the leading-edge midpoint gives  $\Delta_{LE} \sim 4.2\text{--}4.5$  meV for all bands, yielding  $2\Delta_{LE}/k_B T_c \sim 5.5\text{--}6$ , which is reduced compared to results deduced from the peak position, but remains beyond the weak-coupling region. Our observation of a large  $2\Delta/k_B T_c$  ratio and the unusual temperature dependence of the SC gap in  $\text{NaFe}_{0.95}\text{Co}_{0.05}\text{As}$  strongly suggest unconventional superconductivity in this material.

#### IV. CONCLUSION

To summarize, we performed an ARPES study on  $\text{NaFe}_{0.95}\text{Co}_{0.05}\text{As}$ , a material presenting a natural and nonpolar cleaving plane with no expected surface reconstruction. We have shown that  $\text{NaFe}_{0.95}\text{Co}_{0.05}\text{As}$  has a FS topology, a SC gap size, and a SC gap symmetry similar to those of the 122 system, suggesting that inter-FS scattering might be an important parameter for superconductivity in this material. Moreover, the SC quasiparticle peaks and gaps show unusual temperature dependence, similar to that in underdoped cuprates, indicating an unconventional pairing mechanism.

#### ACKNOWLEDGMENTS

We acknowledge useful discussions with Ziqiang Wang, Jiangping Hu, and Weiqiang Yu. The work was supported by the grants from the Chinese Academy of Sciences (2010Y1JB6), Ministry of Science and Technology of China (2010CB923000, 2007CB925001), and the Chinese National Science Foundation (10774189, 11004232 and 11050110422), and the JSPS, TRiP-JST, the MEXT of Japan, CREST-JST and National Science Foundation (Contract No. DE-AC02-05CH11231). The Synchrotron Radiation Center, Madison, WI is supported by the National Science Foundation under Award No. DMR-0537588.

\*scw@ruc.edu.cn

<sup>1</sup>Y. Kamihara, T. Watanabe, M. Hirano, and H. Hosono, *J. Am. Chem. Soc.* **130**, 3296 (2008).

<sup>2</sup>A. V. Chubukov, D. V. Efremov, and I. Eremin, *Phys. Rev. B* **78**, 134512 (2008).

<sup>3</sup>S. Raghu, X.-L. Qi, C.-X. Liu, D. J. Scalapino, and S.-C. Zhang, *Phys. Rev. B* **77**, 220503 (2008).

<sup>4</sup>M. Daghofer, A. Moreo, J. A. Riera, E. Arrigoni, D. J. Scalapino, and E. Dagotto, *Phys. Rev. Lett.* **101**, 237004 (2008).

<sup>5</sup>P. Szabó, Z. Pribulová, G. Pristáš, S. L. Bud'ko, P. C. Canfield, and P. Samuely, *Phys. Rev. B* **79**, 012503 (2009).

<sup>6</sup>K. Hashimoto, M. Yamashita, S. Kasahara, Y. Senshu, N. Nakata, S. Tonegawa, K. Ikada, A. Serafin, A. Carrington, T. Terashima, H. Ikeda, T. Shibauchi, and Y. Matsuda, *Phys. Rev. B* **81**, 220501 (2010).

<sup>7</sup>Y. Nakai, T. Iye, S. Kitagawa, K. Ishida, S. Kasahara, T. Shibauchi, Y. Matsuda, and T. Terashima, *Phys. Rev. B* **81**, 020503 (2010).

- <sup>8</sup>C. W. Hicks, T. M. Lippman, M. E. Huber, J. G. Analytis, J.-H. Chu, A. S. Erickson, I. R. Fisher, and K. A. Moler, *Phys. Rev. Lett.* **103**, 127003 (2009).
- <sup>9</sup>J.-P. Reid, M. A. Tanatar, X. G. Luo, H. Shakeripour, N. Doiron-Leyraud, N. Ni, S. L. Bud'ko, P. C. Canfield, R. Prozorov, and L. Taillefer, *Phys. Rev. B* **82**, 064501 (2010).
- <sup>10</sup>L. Malone, J. D. Fletcher, A. Serafin, A. Carrington, N. D. Zhigadlo, Z. Bukowski, S. Katrych, and J. Karpinski, *Phys. Rev. B* **79**, 140501 (2009).
- <sup>11</sup>Y.-M. Xu, Y.-B. Huang, X.-Y. Cui, E. Razzoli, M. Radovic, M. Shi, G.-F. Chen, P. Zheng, N.-L. Wang, C.-L. Zhang, P.-C. Dai, J.-P. Hu, Z. Wang, and H. Ding, *Nat. Phys.* **7**, 198 (2011).
- <sup>12</sup>L. Zhao, H.-Y. Liu, W.-T. Zhang, J.-Q. Meng, X.-W. Jia, G.-D. Liu, X.-L. Dong, G.-F. Chen, J.-L. Luo, N.-L. Wang, W. Lu, G.-L. Wang, Y. Zhou, Y. Zhu, X.-Y. Wang, Z.-Y. Xu, C.-T. Chen, and X.-J. Zhou, *Chin. Phys. Lett.* **25**, 4402 (2008).
- <sup>13</sup>H. Ding, P. Richard, K. Nakayama, K. Sugawara, T. Arakane, Y. Sekiba, A. Takayama, S. Souma, T. Sato, T. Takahashi, Z. Wang, X. Dai, Z. Fang, G. F. Chen, J. L. Luo, and N. L. Wang, *Europhys. Lett.* **83**, 47001 (2008).
- <sup>14</sup>H.-Y. Liu, X.-W. Jia, W.-T. Zhang, L. Zhao, J.-Q. Meng, G.-D. Liu, X.-L. Dong, G. Wang, R.-H. Liu, X.-H. Chen, Z.-A. Ren, W. Yei, G.-C. Che, G.-F. Chen, N.-L. Wang, G.-L. Wang, Y. Zhou, Y. Zhu, X.-Y. Wang, Z.-X. Zhao, Z.-Y. Xu, C.-T. Chen, and X.-J. Zhou, *Chin. Phys. Lett.* **25**, 3761 (2008).
- <sup>15</sup>K. Nakayama, T. Sato, P. Richard, T. Kawahara, Y. Sekiba, T. Qian, G. F. Chen, J. L. Luo, N. L. Wang, H. Ding, and T. Takahashi, *Phys. Rev. Lett.* **105**, 197001 (2010).
- <sup>16</sup>T. Kondo, A. F. Santander Syro, O. Copie, C. Liu, M. E. Tillman, E. D. Mun, J. Schmalian, S. L. Bud'ko, M. A. Tanatar, P. C. Canfield, and A. Kaminski, *Phys. Rev. Lett.* **101**, 147003 (2008).
- <sup>17</sup>S. Li, C. de la Cruz, Q. Huang, G. F. Chen, T.-L. Xia, J. L. Luo, N. L. Wang, and P. Dai, *Phys. Rev. B* **80**, 020504 (2009).
- <sup>18</sup>S. V. Borisenko, V. B. Zabolotnyy, D. V. Evtushinsky, T. K. Kim, I. V. Morozov, A. N. Yaresko, A. A. Kordyuk, G. Behr, A. Vasiliev, R. Follath, and B. Büchner, *Phys. Rev. Lett.* **105**, 067002 (2010).
- <sup>19</sup>D. S. Inosov, J. S. White, D. V. Evtushinsky, I. V. Morozov, A. Cameron, U. Stockert, V. B. Zabolotnyy, T. K. Kim, A. A. Kordyuk, S. V. Borisenko, E. M. Forgan, R. Klingeler, J. T. Park, S. Wurmehl, A. N. Vasiliev, G. Behr, C. D. Dewhurst, and V. Hinkov, *Phys. Rev. Lett.* **104**, 187001 (2010).
- <sup>20</sup>R. Sknepnek, G. Samolyuk, Y.-b. Lee, and J. Schmalian, *Phys. Rev. B* **79**, 054511 (2009).
- <sup>21</sup>G.-F. Chen, Z. Li, G. Li, W.-Z. Hu, J. Dong, J. Zhou, X.-D. Zhang, P. Zheng, N.-L. Wang, and J.-L. Luo, *Chin. Phys. Lett.* **25**, 3403 (2008).
- <sup>22</sup>K. Kusakabe and A. Nakanishi, *J. Phys. Soc. Jpn.* **78**, 124712 (2009).
- <sup>23</sup>C. He, Y. Zhang, B. P. Xie, X. F. Wang, L. X. Yang, B. Zhou, F. Chen, M. Arita, K. Shimada, H. Namatame, M. Taniguchi, X. H. Chen, J. P. Hu, and D. L. Feng, *Phys. Rev. Lett.* **105**, 117002 (2010).
- <sup>24</sup>M. Neupane, P. Richard, Y.-M. Xu, K. Nakayama, T. Sato, T. Takahashi, A. V. Federov, G. Xu, X. Dai, Z. Fang, Z. Wang, G.-F. Chen, N.-L. Wang, H.-H. Wen, and H. Ding, *Phys. Rev. B* **83**, 094522 (2011).
- <sup>25</sup>D. R. Parker, M. J. P. Smith, T. Lancaster, A. J. Steele, I. Franke, P. J. Baker, F. L. Pratt, M. J. Pitcher, S. J. Blundell, and S. J. Clarke, *Phys. Rev. Lett.* **104**, 057007 (2010).
- <sup>26</sup>I. I. Mazin, D. J. Singh, M. D. Johannes, and M. H. Du, *Phys. Rev. Lett.* **101**, 057003 (2008).
- <sup>27</sup>K. Kuroki, S. Onari, R. Arita, H. Usui, Y. Tanaka, H. Kontani, and H. Aoki, *Phys. Rev. Lett.* **101**, 087004 (2008).
- <sup>28</sup>F. Wang, H. Zhai, and D.-H. Lee, *Europhys. Lett.* **85**, 37005 (2009).
- <sup>29</sup>V. Cvetkovic and Z. Tesanovic, *Europhys. Lett.* **85**, 37002 (2009).
- <sup>30</sup>M. R. Norman, M. Randeria, H. Ding, and J. C. Campuzano, *Phys. Rev. B* **57**, R11093 (1998).
- <sup>31</sup>H. Ding, J. R. Engelbrecht, Z. Wang, J. C. Campuzano, S.-C. Wang, H.-B. Yang, R. Rogan, T. Takahashi, K. Kadowaki, and D. G. Hinks, *Phys. Rev. Lett.* **87**, 227001 (2001).
- <sup>32</sup>D. L. Feng, D. H. Lu, K. M. Shen, C. Kim, H. Eisaki, A. Damascelli, R. Yoshizaki, J.-i. Shimoyama, K. Kishio, G. D. Gu, S. Oh, A. Andrus, J. O'Donnell, J. N. Eckstein, and Z.-X. Shen, *Science* **289**, 277 (2000).
- <sup>33</sup>Y.-M. Xu, P. Richard, K. Nakayama, T. Kawahara, Y. Sekiba, T. Qian, M. Neupane, S. Souma, T. Sato, T. Takahashi, H.-Q. Luo, H.-H. Wen, G.-F. Chen, N.-L. Wang, Z. Wang, Z. Fang, X. Dai, and H. Ding, *Nat. Commun.* **2**, 392 (2011).
- <sup>34</sup>K. Nakayama, T. Sato, P. Richard, Y.-M. Xu, Y. Sekiba, S. Souma, G. F. Chen, J. L. Luo, N. L. Wang, H. Ding, and T. Takahashi, *Europhys. Lett.* **85**, 67002 (2009).
- <sup>35</sup>K. Seo, B. A. Bernevig, and J. Hu, *Phys. Rev. Lett.* **101**, 206404 (2008).